APL Photonics

High-speed switching of biphoton delays through electro-optic pump frequency modulation

Cite as: APL Photonics 2, 011301 (2017); https://doi.org/10.1063/1.4971313
Submitted: 18 October 2016 . Accepted: 19 November 2016 . Published Online: 08 December 2016

Ogaga D. Odele, Joseph M. Lukens, Jose A. Jaramillo-Villegas, Poolad Imany, Carsten Langrock, Martin M. Fejer, Daniel E. Leaird, and Andrew M. Weiner

High-speed switching of biphoton delays through electro-optic pump frequency modulation

Ogaga D. Odele,[1] Joseph M. Lukens,[2] Jose A. Jaramillo-Villegas,[1,3] Poolad Imany,[1] Carsten Langrock,[4] Martin M. Fejer,[4] Daniel E. Leaird,[1] and Andrew M. Weiner[1,a]

[1]*School of Electrical and Computer Engineering and Purdue Quantum Center, Purdue University, West Lafayette, Indiana 47907, USA*
[2]*Quantum Information Science Group, Oak Ridge National Laboratory, Oak Ridge, Tennessee 37831, USA*
[3]*Facultad de Ingenierías, Universidad Tecnológica de Pereira, Risaralda 660003, Colombia*
[4]*E. L. Ginzton Laboratory, Stanford University, Stanford, California 94305, USA*

(Received 18 October 2016; accepted 19 November 2016; published online 8 December 2016)

The realization of high-speed tunable delay control has received significant attention in the scene of classical photonics. In quantum optics, however, such rapid delay control systems for entangled photons have remained undeveloped. Here for the first time, we demonstrate rapid (2.5 MHz) modulation of signal-idler arrival times through electro-optic pump frequency modulation. Our technique applies the quantum phenomenon of nonlocal dispersion cancellation along with pump frequency tuning to control the relative delay between photon pairs. Chirped fiber Bragg gratings are employed to provide large amounts of dispersion which result in biphoton delays exceeding 30 ns. This rapid delay modulation scheme could be useful for on-demand single-photon distribution in addition to quantum versions of pulse position modulation. [http://dx.doi.org/10.1063/1.4971313]

Time-frequency entangled photon pairs ("biphotons") can exhibit strong correlations in both the spectral and temporal degrees of freedom. Such nonclassical states have been touted as applicable for quantum communication, computation, metrology, and optical coherence tomography (OCT).[1–4] For example, large-alphabet quantum key distribution based on arrival-time measurements of entangled photons has been proposed and demonstrated in multiple configurations.[5–9] Biphoton timing measurements can also be used to increase the accuracy of positioning schemes and for distant clock synchronization.[10–12] Yet the availability of programmable optical delay lines would enhance complete control over timing measurements using entangled photons. Ideally, such delay lines should have the capacity for high-speed switching over a wide range of delays.

In the specific application of an on-demand single-photon source, a flurry of recent experiments[13–16] have exploited active temporal switching to synthesize photons from multiple time bins; these examples employ free-space or fiberized switches to route a particular photon through the desired delay line. On the other hand, in classical photonics, tremendous progress has been made in alternative dispersion-based delay systems, with switching speeds approaching the GHz regime.[17–22] Unlike configurations based on discrete delay lines, this approach uses frequency switching followed by a fixed amount of dispersion to produce optical delays which are not only continuously tunable but also intrinsically stable, utilizing a single spatial mode.

In this letter, we demonstrate such a dispersion-based (rather than delay-line-based) approach to realize a high-speed biphoton switch. For the first time, we show MHz switching of biphoton delays through electro-optic pump frequency modulation. Our work draws on a previously proposed idea[23] in which we apply the quantum concept of nonlocal dispersion cancellation[24] alongside pump

[a]Electronic mail: amw@purdue.edu

frequency tuning to furnish the relative signal-idler delay while minimizing distortion of the biphoton time correlation function itself. However, while the delays in Ref. 23 were limited to a few picoseconds and relied on a local detection scheme to measure the correlation function, here we target much longer delays which are resolvable even with high-jitter single-photon detectors, thus allowing for truly nonlocal measurements. Using chirped fiber Bragg gratings (CFBGs) to supply the dispersion in our experiment, we produce a delay range spanning several tens of nanoseconds, five orders of magnitude longer than the initial biphoton correlation width, and two orders of magnitude beyond the jitter-limited temporal resolution. Additionally, we report the largest observed spreading-to-despreading factor for a stretched and compressed biphoton temporal correlation time (>100). In this way we realize both requirements of an ideal delay system—fast switching and long delays—in a technique extendable to GHz switching speeds and compatible with continuous tuning.

The probability distribution of the relative delay for a time-stationary two-photon entangled state is proportional to the Glauber second-order correlation function, $G^{(2)}(\tau) = |\psi(\tau)|^2$, where $\psi(\tau)$ is the biphoton wavepacket and $\tau = t_s - t_i$ denotes the signal-idler delay. For biphotons that are undispersed and obtained through spontaneous parametric down-conversion (SPDC) of a continuous-wave (CW) pump,

$$\psi(\tau) \propto \int d\Omega\, \phi(\Omega) e^{-i\Omega\tau}, \tag{1}$$

where Ω is the signal frequency offset from the center, ω_0, and $\phi(\Omega)$ is the complex biphoton spectrum determined by phase matching in the nonlinear medium. Equation (1) reveals that in the absence of dispersion, the temporal correlation is given by the square modulus of the Fourier transform of the two-photon spectrum. For the type-0 SPDC used in our experiments, the biphotons have a spectral width of ~40 nm which results in a correlation time of ~200 fs, previously measured using sum-frequency generation, as jitter-limited single-photon detectors are unable to resolve such fast coincidences.[25] Propagating the two photons through dispersion introduces phase factors $\exp[i\Phi_s(\Omega)]$ and $\exp[i\Phi_i(-\Omega)]$ under the integral in Eq. (1). Following the discussion in Ref. 23, a shift of $\delta\omega$ in the biphoton central frequency, accompanied by the application of second-order phases $\Phi_s(\Omega) = A\Omega^2/2$ to the signal photon and $\Phi_i(-\Omega) = -A\Omega^2/2$ to the idler photon, will give rise to a biphoton wavepacket of the form,

$$\psi(\tau) \propto \int d\Omega\, \phi(\Omega) e^{-i\Omega(\tau - 2A\delta\omega)}, \tag{2}$$

thereby ensuring a replica of the original shape of $G^{(2)}(\tau)$, along with an additional delay of $2A\delta\omega$. Therefore, by modulating the pump frequency, one can rapidly switch between distinct biphoton delays, analogously to classical pulse position modulation. Indeed, the speed of such switching is limited by the requirement of dispersion cancellation; that is, the pump gate period cannot be smaller than the group delay spread, or cancellation will not occur. Specifically, for a switching period T and biphoton bandwidth Ω_B, one must satisfy $A\Omega_B \ll T$ for ideal performance, a fundamental trade-off important in system design. We also note that Eq. (2) excludes higher-order dispersion coefficients which distort the correlation shape, a nonideality noticeable in some of our results.

We present the general framework of our experiment in Fig. 1. A pump beam—either from a single tunable CW laser or a wavelength switch between two CW lasers—is coupled into a 67-mm-long quasi-phase-matched (QPM) lithium niobate waveguide for frequency doubling. Quasi-phase matching with a periodically modulated second-order nonlinearity can yield very efficient wavelength conversion but only over a narrow bandwidth. In order to accommodate multiple pump wavelengths as efficiently as possible, our QPM grating was fabricated with a continuous phase-modulated poling pattern,[26] giving roughly equal up-conversion efficiency at five distinct bands—the second-harmonic generation (SHG) efficiency of one such waveguide as a function of pump wavelength is shown in Fig. 1. Unconverted pump photons are filtered out and the frequency-doubled beam is coupled into another QPM waveguide for SPDC, producing degenerate and co-polarized entangled photons with a bandwidth of ~40 nm and center frequency equal to that of the pump laser. The phase-matching peaks of the first waveguide are spectrally aligned with those of the second waveguide through temperature control. After filtering the residual frequency-doubled beam, the biphotons are coupled into optical fiber and then separated into two arms with a 50/50 beam splitter; 50% of the time, the photons will exit along different paths and can contribute to coincident arrivals. (Such postselection could be

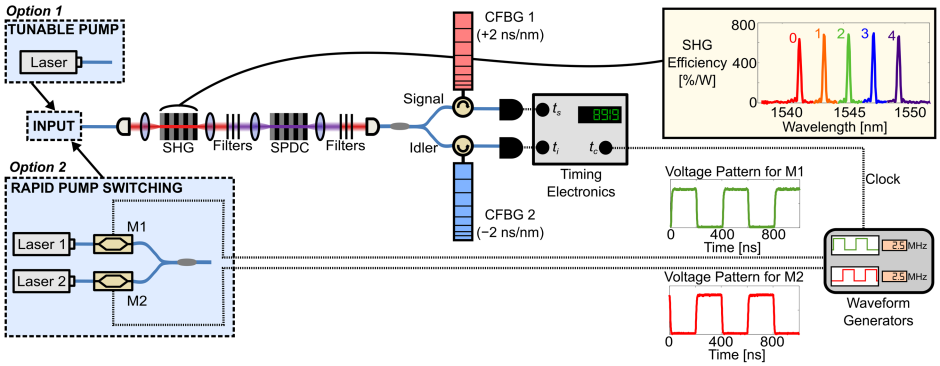

FIG. 1. Experimental setup. Boxes at the input show two types of pump sources—a single tunable CW laser and a rapid wavelength switch (two lasers with intensity modulators M1 and M2 driven synchronously). The input beam is first upconverted in the SHG waveguide and then down-converted in the SPDC waveguide. The CFBGs apply dispersion to the separated signal and idler photons, which are measured by a pair of single-photon detectors. The timing electronics tag the arrival time of each photon, as well as the clock signal from the waveform generators.

avoided, e.g., with a type-II or noncollinear source; our delay method applies equally well to any spectrally entangled source, regardless of preparation.)

One of the output arms of the beam splitter is linked to CFBG 1 with a dispersion parameter of +2 ns/nm (A = 2580 ps^2), while the other output arm is connected to CFBG 2 with a dispersion parameter of −2 ns/nm (A = −2580 ps^2); each CFBG has a loss of only 3 dB, compared to the 24 dB expected from an SMF-28e fiber link with the same dispersion. In addition to their large dispersion, these CFBGs also have a 40-nm-wide acceptance bandwidth that matches the 1530-1570 nm lightwave C band. A pair of gated InGaAs single-photon detectors (Aurea SPD_AT_M2)—each with a quantum efficiency of 20%, a dark count probability per gate of 6×10^{-6}/ns, and a deadtime of 1 μs—are internally triggered, and time-tagging electronics (PicoQuant HydraHarp 400) are then used to retrieve the arrival-time correlations of the biphotons. We note that since these CFBGs are factory components designed to mimic (CFBG 1) and exactly cancel (CFBG 2) 120 km of SMF-28e, they intentionally impart higher-order phase terms: CFBG 1 introduces a cubic phase coefficient of −16.3 ps^3 and CFBG 2 of 15.4 ps^3. Because opposite signs of cubic phase add rather than cancel for spectrally anticorrelated photons,[25] these high-order terms introduce slight distortion in the measured correlation functions below. We emphasize that this would be removed entirely by custom-built CFBGs contributing only the second-order phase.

As a start, we show the extent to which we can spread and compress the biphoton temporal correlation. Our pump here is a single tunable CW laser with wavelength set to 1541 nm, while the power is set such that each detector registers a count rate around 9000 s^{-1} to obtain a coincidence-to-accidental ratio of ~50. Figure 2(a) shows the resulting coincidence peak directly after the 50/50 splitter (after subtracting the background accidentals) with a detector-jitter-limited full width at half maximum (FWHM) of 350 ps; a bin size of 256 ps was used for the plot, and we normalize such that

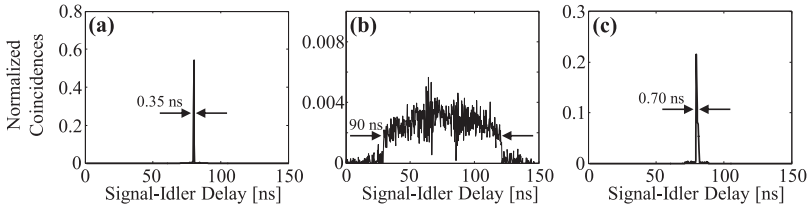

FIG. 2. Spreading, compression of biphoton coincidences. Measured temporal correlation: (a) before applying dispersion, (b) with positive dispersion applied to signal and idler, (c) with positive dispersion on signal and negative on idler. For (a) and (c), the detectors were operated with a 10-ns gate and internally triggered at 1.25 MHz, while for (b), the detectors were operated with a 100-ns gate and triggered at 0.63 MHz.

the sum over all bins adds up to 1. To see the effect of dispersion, we place CFBG 1 in the path of the entangled photons before splitting them into separate arms and detecting them—this is equivalent to sending the signal and idler photons through separate CFBGs with equal dispersion. Since the CFBG cuts off the 1541-nm-centered biphoton at 1530 nm, only signal and idler photons within 1530-1552 nm (a 22 nm bandwidth) contribute to coincidence counts. The broadened correlation is given in Fig. 2(b), showing biphoton wavepacket spreading up to 90 ns. However, when we send the signal photons through CFBG 1 and the idler photons through CFBG 2, we are able to observe nonlocal dispersion cancellation as evidenced in Fig. 2(c). A FWHM of 700 ps is measured for the compressed correlation peak, limited by the residual cubic dispersion of the CFBGs. Our spreading-to-despreading factor of 129 is the largest ever observed for *nonlocal* detection of dispersion cancellation, completely eclipsing the single-digit factors in previous examples.[9,27]

Next, keeping the configuration for nonlocal dispersion cancellation, we show the range of reconfigurable signal-idler delays attainable in our experiment. Using the phase-matching curve (shown in Fig. 1) as a guide, we tune the pump wavelength from 1541 nm to {1543, 1545, 1547, 1549} nm for shifts of {−250, −500, −750, −1000} GHz in the biphoton center frequency. The coincidence patterns are given in Fig. 3, showing temporal shifts of {0, 8, 16, 24, 32} ns; the error bars represent the standard deviation over five acquisitions. Excellent agreement can be seen between our experimental results [Fig. 3(a)] and the theoretical predictions [Fig. 3(b)]. The correlation peaks broaden as the center wavelength approaches 1550 nm due to a combination of the cubic dispersion and transmission response of our CFBGs (both effects were accounted for in the numerical simulations). The closer the biphoton center wavelength is to 1550 nm, the larger the biphoton bandwidth transmitted through the CFBG, which yields a more pronounced effect of the uncompensated cubic spectral phase on the temporal correlation. Additionally, continuous delay control would be realizable with only minor modifications to the present configuration. In our case, the permissible pump frequencies—and hence biphoton delays—are fixed to discrete values by the waveguide phase matching (Fig. 1 inset). Yet nonlinear media offering a broadband region of low phase mismatch would instead permit delay control over a continuum of pump wavelengths. Such would be the case with, e.g., a short nonlinear crystal or a QPM waveguide with a chirped poling pattern, where in general one compromises between peak nonlinear efficiency and total bandwidth.[28]

Lastly, we demonstrate rapid delay modulation of different signal-idler delay combinations by implementing a wavelength switch which consists of two electro-optic intensity modulators (EOSpace) and two tunable CW lasers operating at distinct wavelengths. The modulators are driven with a pair of synchronized waveform generators, both outputting 50%-duty-cycle square pulses with a period of 400 ns (2.5 MHz frequency), but one phase-shifted from the other by half a period, as shown in Fig. 1; when M1 is high, M2 is low, and vice versa. The detectors are again triggered by an independent 1.25 MHz clock which, because of its asynchronicity with these modulation patterns, allows the detectors to evenly sample the full switching period. In addition to tagging the signal and idler arrival times, we also record the clock signal from the wavelength switch, enabling us to experimentally corroborate the pump wavelength responsible for each coincidence event.

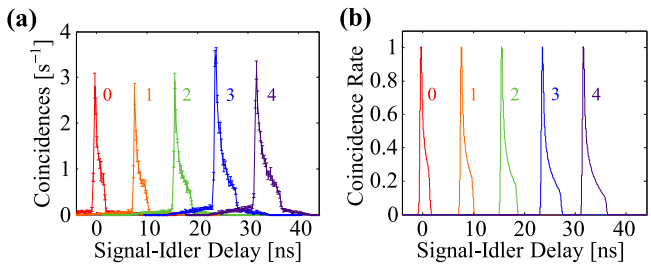

FIG. 3. Delay tuning of biphoton coincidences. (a) Experimental and (b) theoretical correlation functions corresponding to the pump wavelength detuned by $\{0, 1, 2, 3, 4\} \times (-250\ \text{GHz})$. The detectors used to obtain (a) were operated with a 10-ns gate and triggered at 1.25 MHz.

The result for modulating the pump wavelength between 1545 nm and 1549 nm is presented in Fig. 4(a)—we plot photon coincidences as a function of both signal-idler delay ($t_s - t_i$) and signal-clock delay ($t_s - t_c$). On the signal-idler delay axis, the coincidences cluster at 16 ns and 32 ns, respectively. Moreover, as expected from the wavelength modulation at 2.5 MHz, we see that the coincidences due to the 1545-nm pump appear between 200 and 400 ns on the signal-clock delay axis while the coincidences due to the 1549-nm pump turn out between 0 and 200 ns. Similarly, we obtain the result in Fig. 4(b) for wavelength modulation between 1543 nm and 1549 nm; the signal-idler delays corresponding to the two different wavelengths again appear in separate halves of the signal-clock delay axis. The slight overlap between coincidence events recorded in the first and second halves of the clock period [in Figs. 4(a) and 4(b)] only occurs because our group delay spread is starting to approach the pump gate period. And so our results show the first high-speed modulation of biphoton delays.

Our delay control mechanism has the potential to positively impact several applications. For example, it could be used for on-the-fly delay correction and mitigating delay fluctuations in quantum networks—including clock synchronization and quantum communication networks. In the case of single-photon sources, this approach could be applied toward fast temporal multiplexing. For although our demonstration here concentrated on pump frequency tuning, one could also employ frequency shifting of heralded single photons directly. In this way, one dispersive medium—rather than active switches and fixed delay lines[13–15]—would impart the tunable delay required in temporally multiplexed single-photon sources. A second frequency converter at the output can then be used to remove the initial wavelength shift, thereby making our approach fully compatible with the need for frequency indistinguishability while simultaneously exploiting spectrally dependent delay.

In summary, we have demonstrated delay tuning of biphotons up to 32 ns through pump frequency tuning. This ratifies our tunable delay scheme[23] as a robust method not only for ps delays but also for ultralong ns separations. We also presented our results on modulating biphoton arrival times at a rate of 2.5 MHz. Moreover, the technique applies well to essentially any desired switching speed, so long as the modulated pump remains within the acceptance bandwidth of the nonlinear process. For example, GHz switching speeds could be reached in our setup with faster electronics and reduced

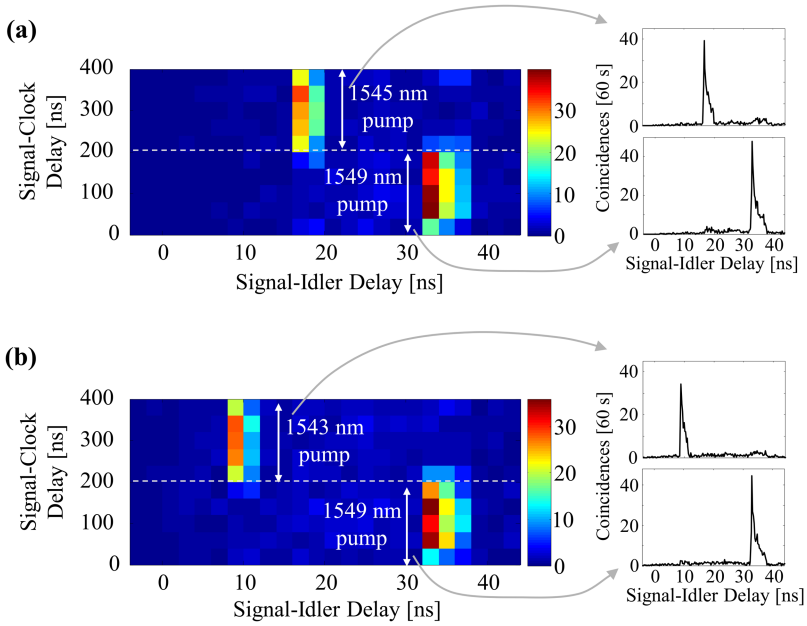

FIG. 4. Rapid delay modulation results with coincidences plotted as a function of signal-idler delay (horizontal axis) and signal-clock delay (vertical axis). (a) Modulation between 1545 and 1549 nm pump wavelengths. (b) Modulation between 1543 and 1549 nm pump wavelengths. The insets show the total coincidences integrated over the signal-clock delays of 200-400 ns (top) and 0-200 ns (bottom). The detectors used in these measurements were operated with a 30-ns gate.

total dispersion: this would effectively rescale the temporal axis but otherwise preserve performance. Such flexibility implies an assortment of design opportunities, so that it would also be interesting to examine this technique as a possible degree of freedom in novel quantum key distribution protocols, such as quantum analogues of pulse position modulation.

This work was funded by the National Science Foundation under Grant No. ECCS-1407620 and performed in part at Oak Ridge National Laboratory, operated by UT-Battelle for the U.S. Department of Energy under Contract No. DE-AC05-00OR22725. J.A.J. acknowledges support from Colciencias Colombia through the Francisco Jose de Caldas Conv. 529 scholarship and Fullbright Colombia. We thank Sandeep Baskar for assistance with the wavelength switch.

[1] N. Gisin, G. Ribordy, W. Tittel, and H. Zbinden, "Quantum cryptography," Rev. Mod. Phys. **74**, 145–195 (2002).
[2] C. H. Bennett and D. P. DiVincenzo, "Quantum information and computation," Nature **404**, 247–255 (2000).
[3] V. Giovannetti, S. Lloyd, and L. Maccone, "Advances in quantum metrology," Nat. Photonics **5**, 222–229 (2011).
[4] M. B. Nasr, B. E. A. Saleh, A. V. Sergienko, and M. C. Teich, "Demonstration of dispersion-canceled quantum-optical coherence tomography," Phys. Rev. Lett. **91**, 083601 (2003).
[5] I. Ali Khan and J. C. Howell, "Experimental demonstration of high two-photon time-energy entanglement," Phys. Rev. A **73**, 031801 (2006).
[6] I. Ali-Khan, C. J. Broadbent, and J. C. Howell, "Large-alphabet quantum key distribution using energy-time entangled bipartite states," Phys. Rev. Lett. **98**, 060503 (2007).
[7] J. Nunn, L. J. Wright, C. Söller, L. Zhang, I. A. Walmsley, and B. J. Smith, "Large-alphabet time-frequency entangled quantum key distribution by means of time-to-frequency conversion," Opt. Express **21**, 15959–15973 (2013).
[8] J. Mower, Z. Zhang, P. Desjardins, C. Lee, J. H. Shapiro, and D. Englund, "High-dimensional quantum key distribution using dispersive optics," Phys. Rev. A **87**, 062322 (2013).
[9] C. Lee, Z. Zhang, G. R. Steinbrecher, H. Zhou, J. Mower, T. Zhong, L. Wang, X. Hu, R. D. Horansky, V. B. Verma, A. E. Lita, R. P. Mirin, F. Marsili, M. D. Shaw, S. W. Nam, G. W. Wornell, F. N. C. Wong, J. H. Shapiro, and D. Englund, "Entanglement-based quantum communication secured by nonlocal dispersion cancellation," Phys. Rev. A **90**, 062331 (2014).
[10] V. Giovannetti, S. Lloyd, and L. Maccone, "Quantum-enhanced positioning and clock synchronization," Nature **412**, 417–419 (2001).
[11] V. Giovannetti, S. Lloyd, L. Maccone, and F. N. C. Wong, "Clock synchronization with dispersion cancellation," Phys. Rev. Lett. **87**, 117902 (2001).
[12] A. Valencia, G. Scarcelli, and Y. Shih, "Distant clock synchronization using entangled photon pairs," Appl. Phys. Lett. **85**, 2655–2657 (2004).
[13] F. Kaneda, B. G. Christensen, J. J. Wong, H. S. Park, K. T. McCusker, and P. G. Kwiat, "Time-multiplexed heralded single-photon source," Optica **2**, 1010–1013 (2015).
[14] G. J. Mendoza, R. Santagati, J. Munns, E. Hemsley, M. Piekarek, E. Martín-López, G. D. Marshall, D. Bonneau, M. G. Thompson, and J. L. O'Brien, "Active temporal and spatial multiplexing of photons," Optica **3**, 127–132 (2016).
[15] C. Xiong, X. Zhang, Z. Liu, M. J. Collins, A. Mahendra, L. G. Helt, M. J. Steel, D.-Y. Choi, C. J. Chae, P. H. W. Leong, and B. J. Eggleton, "Active temporal multiplexing of indistinguishable heralded single photons," Nat. Commun. **7**, 10853 (2016).
[16] R. J. A. Francis-Jones, R. A. Hoggarth, and P. J. Mosley, "All-fibre multiplexed source of high-purity heralded single photons," Optica **3**, 1270–1273 (2016).
[17] V. Torres-Company, J. Lancis, and P. Andrés, in *Progress in Optics*, edited by E. Wolf (Elsevier, 2011), Vol. **56**, Ch. 1, pp. 1–80.
[18] J. van Howe and C. Xu, "Ultrafast optical delay line by use of a time-prism pair," Opt. Lett. **30**, 99–101 (2005).
[19] J. van Howe and C. Xu, "Ultrafast optical delay line using soliton propagation between a time-prism pair," Opt. Express **13**, 1138–1143 (2005).
[20] J. van Howe and C. Xu, "Ultrafast optical signal processing based upon space-time dualities," J. Lightwave Technol. **24**, 2649–2662 (2006).
[21] Y. Wang, C. Yu, L. Yan, A. E. Willner, R. Roussev, C. Langrock, M. M. Fejer, J. E. Sharping, and A. L. Gaeta, "44-ns continuously tunable dispersionless optical delay element using a PPLN waveguide with two-pump configuration, DCF, and a dispersion compensator," IEEE Photon. Technol. Lett. **19**, 861–863 (2007).
[22] Y. Okawachi, M. A. Foster, X. Chen, A. C. Turner-Foster, R. Salem, M. Lipson, C. Xu, and A. L. Gaeta, "Large tunable delays using parametric mixing and phase conjugation in Si nanowaveguides," Opt. Express **16**, 10349–10357 (2008).
[23] O. D. Odele, J. M. Lukens, J. A. Jaramillo-Villegas, C. Langrock, M. M. Fejer, D. E. Leaird, and A. M. Weiner, "Tunable delay control of entangled photons based on dispersion cancellation," Opt. Express **23**, 21857–21866 (2015).
[24] J. D. Franson, "Nonlocal cancellation of dispersion," Phys. Rev. A **45**, 3126–3132 (1992).
[25] J. M. Lukens, A. Dezfooliyan, C. Langrock, M. M. Fejer, D. E. Leaird, and A. M. Weiner, "Demonstration of high-order dispersion cancellation with an ultrahigh-efficiency sum-frequency correlator," Phys. Rev. Lett. **111**, 193603 (2013).
[26] M. Asobe, O. Tadanaga, H. Miyazawa, Y. Nishida, and H. Suzuki, "Multiple quasi-phase-matched $LiNbO_3$ wavelength converter with a continuously phase-modulated domain structure," Opt. Lett. **28**, 558–560 (2003).
[27] S.-Y. Baek, Y.-W. Cho, and Y.-H. Kim, "Nonlocal dispersion cancellation using entangled photons," Opt. Express **17**, 19241–19252 (2009).
[28] D. S. Hum and M. M. Fejer, "Quasi-phasematching," C. R. Phys. **8**, 180–198 (2007).